

Article citation info:

Warczek J, Żak K, The assessment of the technical condition of a tire belt using computed tomography, *Eksploracja i Niezawodność – Maintenance and Reliability* 2024; 26(2) <http://doi.org/10.17531/ein/183177>

The assessment of the technical condition of a tire belt using computed tomography

Indexed by:



Jan Warczek^{a,*}, Krzysztof Żak^b

^a Silesian University of Technology, Poland

^b Opole University of Technology, Poland

Highlights

- The paper presents the possibilities of testing tires with the use of computed tomography.
- The authors demonstrated the possibility of a detailed analysis of composite structures.
- The proposed method allows for the assessment of operational damage to car tire belts.

Abstract

Car tire belting is a key structural element. Its operation in the tire determines the maintenance of the geometrical stability of the pneumatic wheel in conditions of variable operational loads. The belt creates

a spatial composite structure in which the structural component is usually made of braided steel strands. The even arrangement of the fibers in the belt determines its mechanical properties. Under normal conditions, the belting is invisible in used tires and its technical condition is difficult to assess. The arrangement of the belt wires in the tire can be seen using X-ray imaging, which was used in this work. In the conducted research, various configurations of the lamp settings and the detector of the measurement system were tested. On the basis of the tests performed, it is possible to assess irregularities in the belting resulting from manufacturing errors. However, a more important application of the obtained results is the possibility of assessing operating wear. Delamination in the belt detected during the tests reduce the safety of using such tires.

Keywords

car tire, computed tomography, operational damage tests

This is an open access article under the CC BY license (<https://creativecommons.org/licenses/by/4.0/>)

1. Introduction

When driving, the face of the tire adheres to the road surface in the form of a flat contact surface. The tire is deformed along the length and width of the tread, which leads to transverse and longitudinal bending of the tire face. Tire deformations are a direct cause of rolling resistance, but at the same time they are an essential factor ensuring the ability to transfer forces and moments between the ground and the car. The main material components of the tire are different grades of rubber compounds, which are responsible for the ability to level

uneven surfaces and create a contact zone. The work of the tire consists in cyclically repeated deformations in the contact zone with the road surface, which lead to energy dissipation. In the construction of car tires, due to the occurrence of variable loads and rotational speeds of the road wheels, it is necessary to use structural elements responsible for maintaining the external geometry. Rubber mixtures without reinforcements would quickly be destroyed leading to geometric deformations. In the circumferential part of the tire, the belt under the tread is responsible for maintaining the

(*) Corresponding author.

E-mail addresses:

J. Warczek (ORCID: 0000-0002-4767-5588) jan.warczek@polsl.pl, K. Żak (ORCID: 0000-0002-0157-3340) k.zak@po.edu.pl

geometric dimensions [7]. The most commonly used construction material for car tire belts is steel, which is evenly distributed around the circumference of the tire in the form of wires (cords) stabilized with a rubber matrix [8]. The sidewalls of the tires are reinforced with fibers made of plastic-based materials or, less commonly, metallic ones. The adherence of the tire bead to the rim is ensured by the use of bead wires in the form of a weave of steel rods [17]. According to these considerations, each tire currently used in motor vehicles is a layered composite structure with a complex external geometry. The internal structure of a typical car tire is shown in Figure 1.

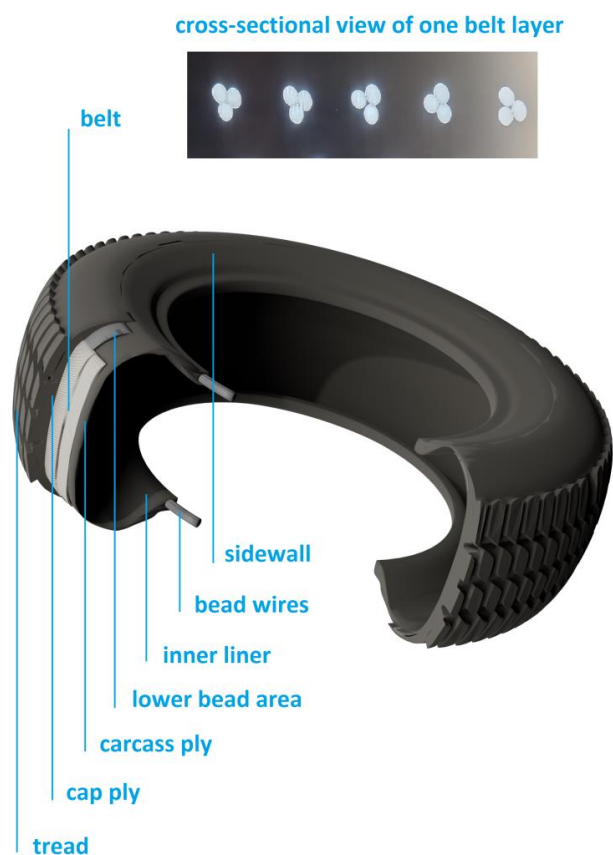


Fig. 1. View of the basic structural elements of the tire and a magnification of the physical cross-section of the belt made by the CT method.

The car tire belt is a structural element that determines the maintenance of the geometrical stability of the pneumatic wheel in conditions of variable loads. The belt is a composite structure in which the structural component is usually made of metal wires. Even distribution of reinforcement in the belt determines its mechanical properties [23]. Under normal operating conditions, the tire belt is invisible and its technical condition is difficult to assess. The location of the belt cords

in the tire can be seen using x-ray imaging, which is one of the basic testing methods. Other alternative non-destructive testing methods of tire belting are also being developed [4, 5].

A particularly important purpose of using x-ray methods is the quality control of products used in production processes. Linear X-ray detector (LDA) arrays have proven to be the ideal choice for non-destructive testing (NDT) in quality control and wear and tear assessment [1, 11]. Digital x-ray detectors have been introduced to tire quality control relatively recently. This solution, based on an intelligent digital platform, which is focused on improving image quality, increases the maximum speed of tire scanning and allows shortening the test time. Typical industrial X-ray imaging systems used in the tire industry are based on a U-shaped detector [27, 28].

Detecting tire belt discrepancies from x-ray images is a task that requires expertise in x-ray assessment. A trained operator is able to detect most non-conformities resulting from manufacturing errors. The problem is the throughput of such analysis, which is limited by the possibilities of human perception [32]. In the case of tire quality control, it is possible only for selected samples from the entire production series. There are specific classes of belting errors that can be recognized by traditional imaging techniques. However, these techniques struggle with complex background textures, external interference, and differences in lighting conditions.

Many articles present various methods of automated recognition of non-conformities in tire construction. Such tasks are performed by using image segmentation methods, object edge detection, image processing using mathematical methods and machine learning. This is inspired by two main factors: the availability of computing power and the rapid digitization of society, which enables the creation of large databases of tagged tire scan samples.

The work [24] proposes a tire defect detection method that uses the similarity of tire image features to detect anomalies. The proposed detection algorithm consists mainly of three stages: a kernel regression description to obtain a set of tire image feature vectors, an evaluation of pixel dissimilarity and estimation by weighted averaging of dissimilarities between one pixel and its neighbors (anomaly detection) and finally, in the thresholding process, detection of discrepancies.

Another method of belting fault detection is end-to-end, which is used to automatically detect tire defects in x-ray images. The described method is based on the periodicity of X-ray images of tires and the Siamese net used as part of the classifier for detecting inconsistencies in belting [34].

In [36], a new tire defect detection model using the Concise Semantic Network (concise ANN) was tested for automatic visual tire inspection.

Another approach to the problem of tire defect detection automation is presented in [13]. In this article, the feature distribution generated by local inverse differential moments (LIDM) is considered as an effective representation of the tire x-ray texture image. The defect feature map (DFM) is constructed by calculating the Hausdorff distance between the LIDM function distributions of the original tire image. The defect detection algorithm is not only resistant to background noise, but also has a greater ability to handle different shapes of defects.

In [30], a comprehensive light semantic segmentation network was proposed for the implementation of bead toe tire defect detection. The texture function of the different areas of the tire is extracted by the encoder. Then the decoder connects the output function of the encoder. When assessing the final effect of image segmentation, the local mIoU index was used.

In the work [35], based on the X-ray image of a tire with a periodic texture, an algorithm for detecting a joint in the belt was proposed, whose incorrect execution is one of quite frequent manufacturing defects.

In the article [15], a new model for detecting contamination defects in X-ray images of tires was proposed. First, a binarization algorithm based on columnar grayscale correction was designed, which can get more details than other algorithms and lay a solid foundation for further detection. Then, the tire X-ray image segmentation algorithm could accurately divide the image of the tire. Finally, two thresholds were used to assess whether there was a contamination defect in the tire image.

In the automatic detection of tire defects, various techniques of the initial x-ray image processing are also used, e.g. based on large-scale wavelet analysis [31].

Automatic tire damage detection has become an important

issue in the tire industry. However, it is difficult to check the internal structure of a tire using surface detection. Therefore, an x-ray image detector is used to inspect tire damage. Currently, the detection of defective tires is ineffective as tire factories often carry out detection by manually checking x-ray images. With the development of deep learning, supervised learning was introduced to replace human resources. However, in real industrial conditions, defective samples are rarely compared to defect-free samples. The number of defective samples is insufficient to isolate supervised feature models and to identify non-qualified products.

In [33], an unsupervised approach was proposed to solve these problems, using samples of undetermined defects for training. In addition, an augmented reconstruction method and a self-supervised training strategy were introduced. In the work [25], the algorithm used was verified by the developed software for automatic tire damage detection in which the desired results were obtained.

To sum up, the methods for automatic detection of non-conformities in the tire construction using x-ray are primarily: Lightweight semantic segmentation network, Faster R-CNN, Unsupervised Learning with Generative Adversarial Network, MobileNet Single Shot MultiBox Detector (MobileNet-SSD), and Lightweight Convolutional Neural Network that is designed for real-time object detection on mobile and embedded devices and YOLO ver. 4 and 5.

All the described methods allow the detection of defects in the construction of a tire on the basis of flat images obtained by x-raying the tires with high-energy radiation. The level of detail of the obtained results allows for efficient detection of tire belt irregularities but has limitations in terms of detecting belt structure destruction caused by operating wear.

In the assessment of damage to the tire belt, factors related to the operation of the drive system and the excitation caused by road unevenness and traffic conditions should be taken into account. An important factor influencing tire loads is the functioning of the drive system, the condition of which can be determined using indirect measurement methods [20]. The method of transmitting power from the engine to the wheels plays an important role in the operational loads of tires [2]. Taking into account the impact of the drive system on tire loads, effective methods of monitoring its technical condition

should also be used [3, 19]. On the other hand, the deterioration of the belt condition translates into travel safety and tire operating conditions in the contact zone. In [16] a method for assessing the stability of vehicle motion based on the analysis of accelerations was presented. In turn, the technical condition of tires translates into their acoustic properties. One method for assessing tire noise is presented in [29]. This paper presents the assumptions and preliminary results of tire belt tests using X-ray tomography. This is a new approach to car tire research that allows for a detailed analysis of the tire's structural component. In the conducted research, various configurations of the lamp settings and the detector of the measurement system were tested. On the basis of the performed tests, it is possible to assess irregularities in the belting resulting from manufacturing errors, but a more important application of the obtained results is the possibility of assessing the operating wear of the belt cords. Operational damage to the belt detected during the tests reduces the safety of using such tires. A huge advantage of this approach to tire research is the ability to assess the spatial structure of tires, which was impossible with classic X-rays.

2. Description of the test method and measurement stand

Computed Tomography (CT) technology, which is an X-ray imaging method widely used mainly in medicine, was used in the tire belt research, co-developed by Allan MacLeod Cormack and Godfrey Newbold Hounsfield. These scientists received the Nobel Prize in 1979 for this achievement [14, 26].

Today, X-ray computed tomography (CT) is used in three different fields. These are the previously mentioned medicine, and since 1980 it has been popularized in material analysis and non-destructive testing (e.g. detection of material defects). Most recently, starting from 2005 CT technology has been used in dimensional metrology, which is an alternative to 3D coordinate measuring machines or measuring arms using contact or optical methods [18].

CT imaging is a type of X-ray spectroscopy. It converts electrical energy (electrons) into X-ray photons which are passed through the object [14]. Then they are measured by a detector and converted back into electrons (whose density is inversely proportional to the density of the object and the change in photon intensity depends on the density of different

parts of the measured object). In order to obtain an image (3D or 2D) of the measured object, the CT machine passes X-ray photons at different angles through the object in the range of 360 degrees [26].

Computed tomography in industry occurs in two configurations [10, 26]. The first one is a cone-beam system (Fig. 2) in which the source of radiation is an X-ray tube with a power of 150 to 450 kV. The scanned object is placed on a table that makes a full 360° rotation, obtaining the entire cross-section of the scanned object.

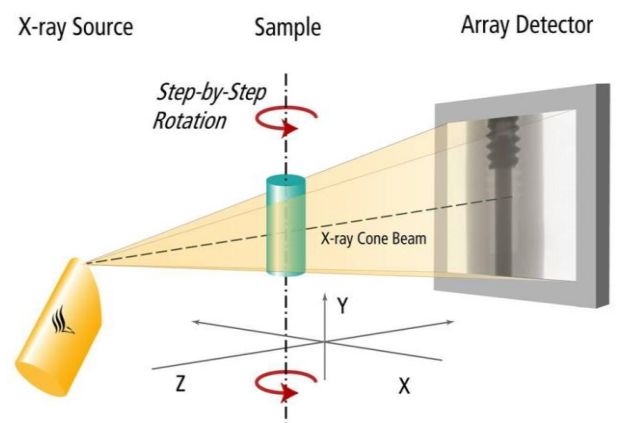


Fig. 2. Scheme of measurement by a computer tomograph using a cone beam system [18].

The second configuration is a parallel-beam system (Fig. 3). A flat beam of X-ray radiation is used here, emitted in the direction of the measured object placed on a turntable. The measured object moves angularly and linearly in the x, y and z directions, or the X-ray tube moves relative to the line detector. As the object moves, the object rotates 360° in each step.

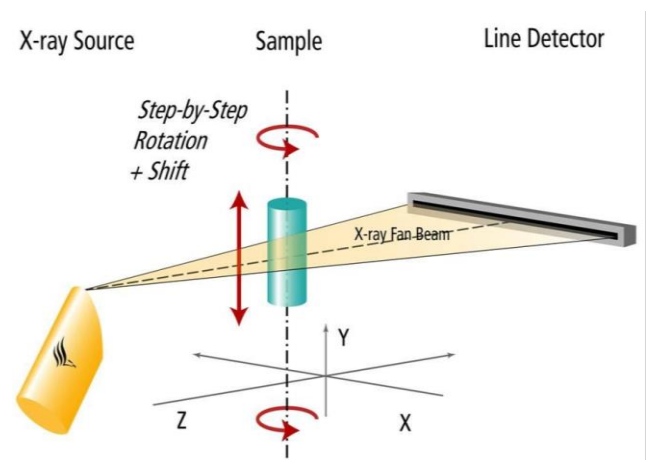


Fig. 3. Scheme of measurement by a computer tomograph using a system with a parallel beam [18].

A very important aspect of a good mapping of the scanned object is the number of projections made during a full rotation of the measured object as well as the size of the focal length [26].

The method of enlarging or reducing the measured object is shown in Fig. 4a. As can be seen, a greater magnification of

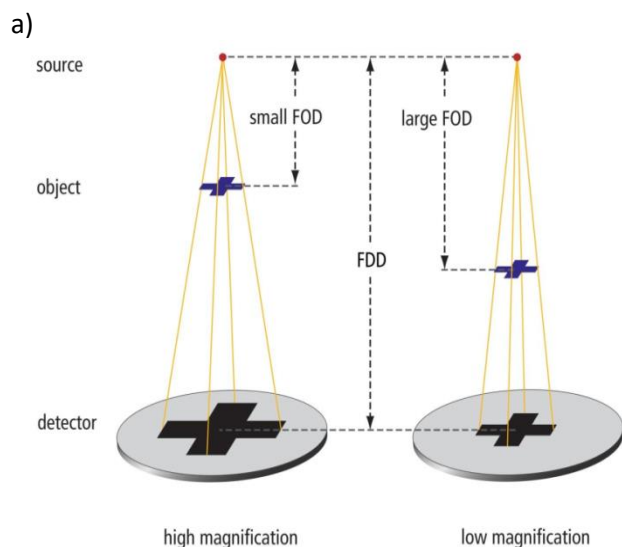


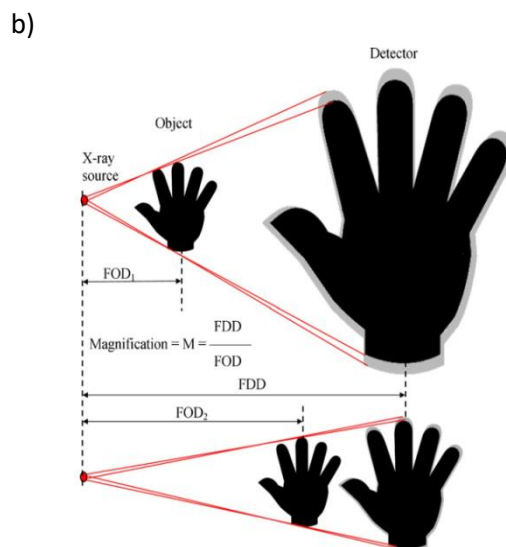
Fig. 4. Image magnification (a) and image blurring effect in computed tomography [10, 18].

In computed tomography, the final effect of imaging (accuracy) depends on the number of projections made during a full rotation of the measured object. The unit of the 3D spatial image is the voxel (volumetric element). Voxel is an anagram of the words "volume" and "pixel", which generally speaking is a unit representing 3D spatial volume data. Another term for a voxel is a 3D pixel. Voxels are almost identical to pixels and have a specific cell inside the grid. However, the main difference is that instead of dealing with two axes, we use three axes here [18].

Computed tomography (CT) technology was used in the tire belt tests, which allows looking inside the structure and creating its 3D representations and cross-sections in any plane (detail imaging). The obtained tire scans in the form of a matrix enable their interpretation in terms of the geometric correctness of details regarding porosity or inclusions, and correlating the obtained results with those obtained using other test methods [12]. In the case of using periodic scanning methods to a limited extent, it is possible to study mechanical interactions in the material (e.g. flow analysis) [6, 9].

The use of computed tomography results for advanced tire information processing techniques allowed, among others:

the measured object can be obtained by bringing the object closer to the source. This action has positive as well as negative effects. The result may be an increase in the resolution of the measured object, but it may cause blurring of the image due to the finite size of the X-ray spot, which is shown in Fig. 4b.



- assessment of geometric compliance,
- analysis of the correctness of the implementation of production processes in terms of structural correctness,
- location and analysis of the distribution and dimensions of defects and non-conformities,
- studying local distribution of belt fibers and their global orientation,
- assessment of structural damage caused by wear or mechanical damage.

By taking a large number of photos of the tested tire, it is possible to obtain 3D images of the belt using dedicated software based on the Radon transform. The Radon transform is a mathematical description of the projection and it can be written as:

$$P_{\phi}(t) = \int_{-\infty}^{\infty} \int_{-\infty}^{\infty} f(x, y) \delta(x \cos \phi + y \sin \phi - t) dx dy \quad (1)$$

where:

- $f(x, y)$ – a function describing the spatial distribution of radiation absorption,
- δ – Dirac delta distribution,
- ϕ – X-ray angle,
- t – shift relative to the center,
- $x \cos \phi, y \sin \phi$ – point coordinates transferred to the

projection coordinate system,

$P_{\phi(t)}$ – value of the projection function for angle ϕ and shift t

Thanks to this, we can obtain spatial images of the details of the internal structure of tires. In the tire tests, the Phoenix

v|tome|x s 240 3D volumetric scanner was used, whose main elements comprising the measurement system are shown in Figure 5.

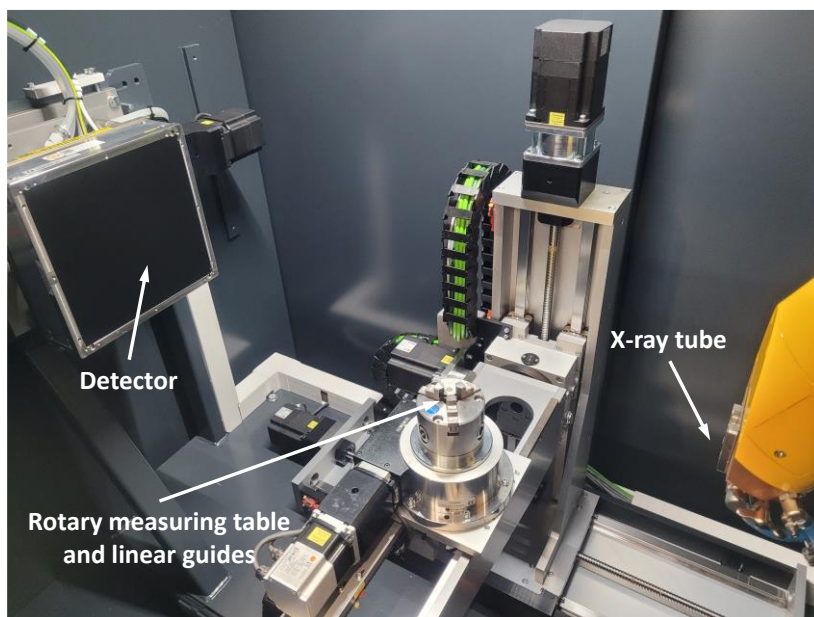


Fig. 5. View of the basic elements of the x-ray imaging system.

A simplified procedure for imaging a tire on a volumetric scanner is presented below (Fig. 6) and in Tab. 1 shows

parameters set while scanning the measured tire.

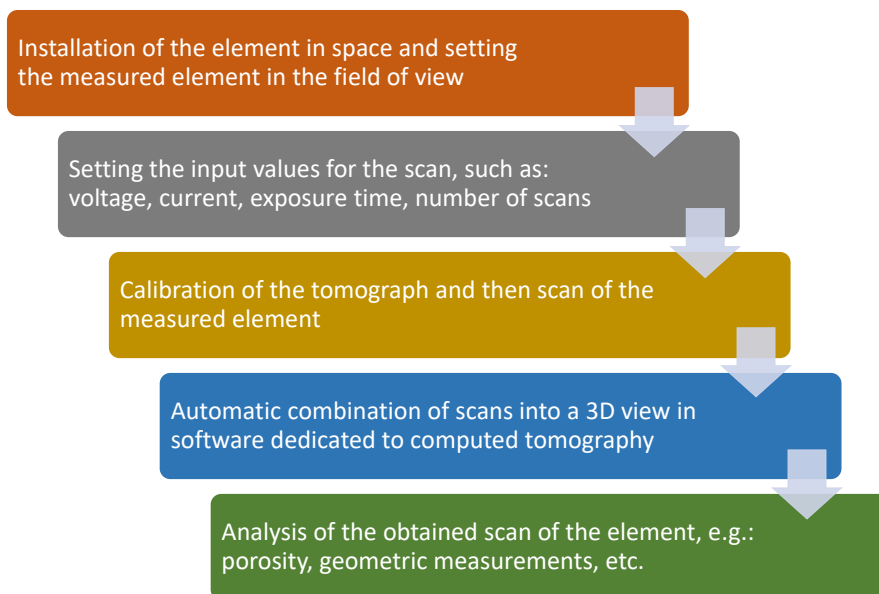


Fig. 6. Simplified diagram of the scanning procedure on a volumetric (CT) scanner.

Tab. 1. Volumetric scanner settings.

<i>parameter</i>	<i>value</i>	<i>physical unit</i>
zoom	1.4	b. w.
the size of one Voxel	142.84	μm
number of photos	1076	b. w.
exposure time	333	ms
voltage	120	kV
current	100	μA

3. The research results and their analysis

The tests were carried out on typical tires used in passenger cars. The design solutions of such tires from different manufacturers show a large range of similarities. In all tested tires there was a metal belt, whose essential element is the

spatial arrangement of steel cords (Fig. 1). One of the typical operating damage to tires is the puncture of the face caused by its penetration by a sharpened indenter. Often, after such damage, the tire is repaired by cleaning the damaged area and then filling it with a rubber compound. During such a repair, it

is impossible to assess to what extent the belt was damaged. In the conducted tests, deliberate damage to the tire was made using various penetrators. The view of the tested tire fragment in three successive test phases is shown in Figure 7.

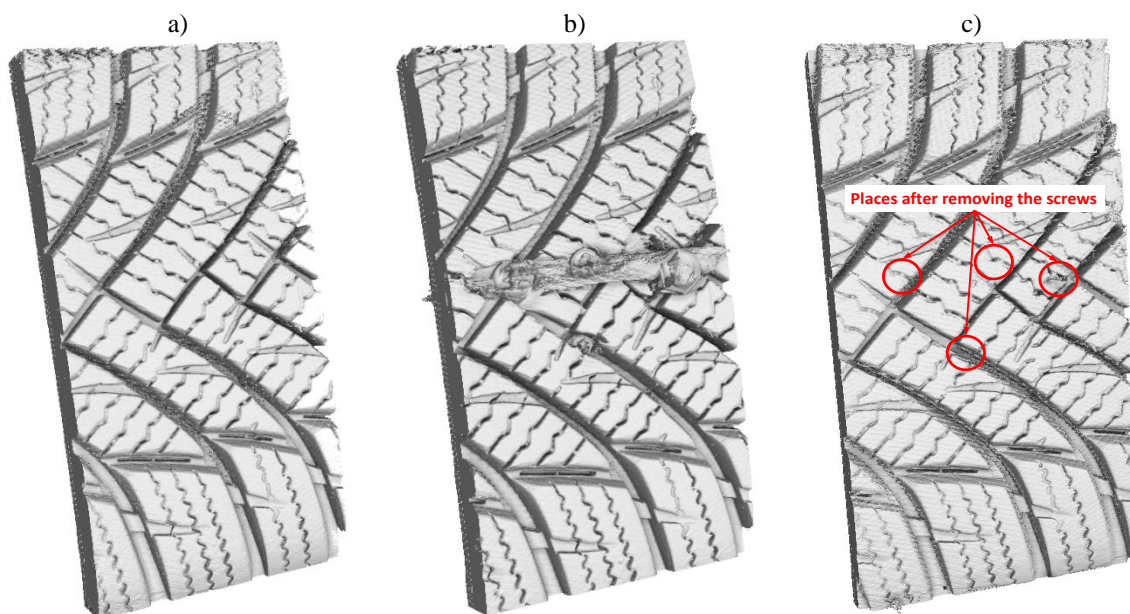


Fig. 7. Image of a fragment of the tread of the tested tire obtained by the Phoenix v|tome|x s 240 3D scanner: a) before damage, b) with inserted penetrators, c) after removing the penetrators (external damage to the rubber layers is visible).

Disturbances visible in Fig. 7b are typical image distortions resulting from dirt or a combination of two different materials, which are sometimes difficult to remove in the post-process. Figure 7 shows images of the outer surface of the tested tire fragment. Similarities can be noticed with the results obtained in surface scanning methods using laser scanners [22], but it has some other features. In the results obtained, it is possible to analyze, for example, surface depressions (grooves of small width and great depth), which

are a typical solution in the construction of a car tire tread. The device used in the tire research allows the imaging of the internal structure of other objects with complex shapes [21].

After performing the CT tests, spatial images of the internal structure of the tested tire were obtained. A view of belt damage caused by external interference and cord placement errors caused by manufacturing defects is shown in Figures 8 and 9.

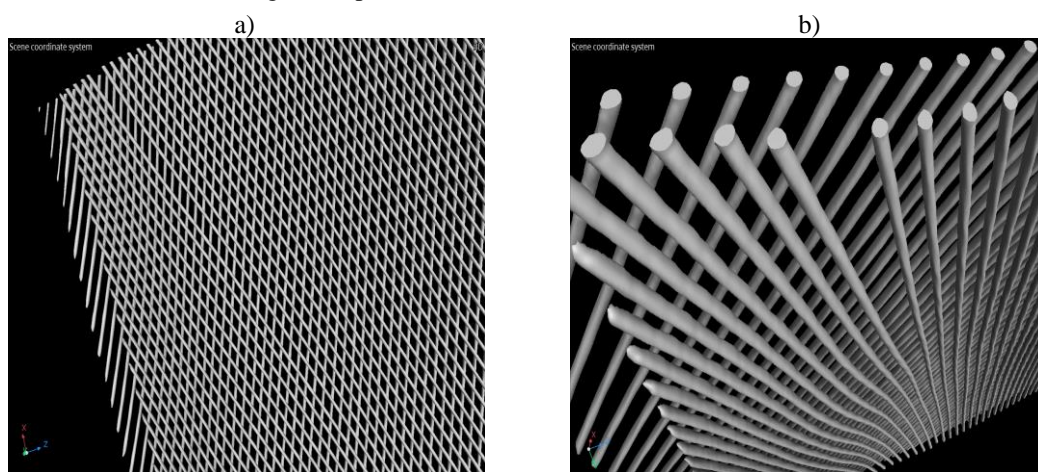


Fig. 8. Image of a fragment of the belt of the tested tire obtained by the Phoenix v|tome|x s 240 volumetric 3D scanner with a visible manufacturing error.

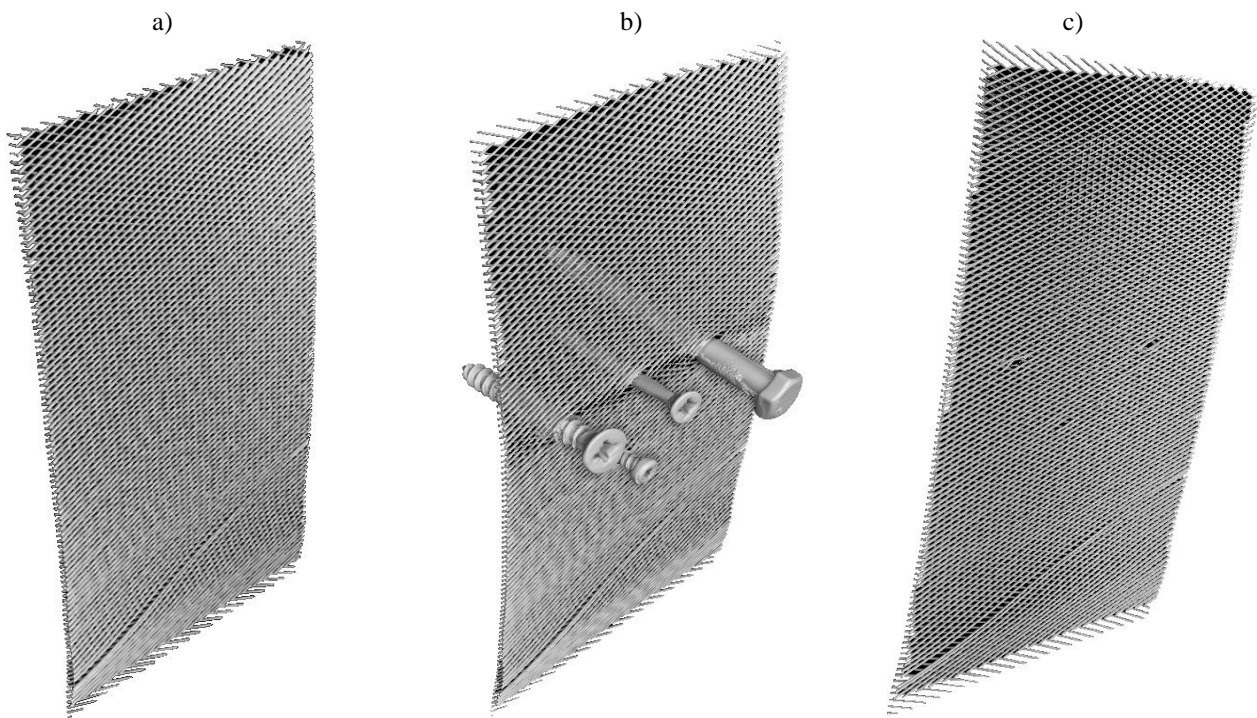


Fig. 9. Image of a fragment of the test tire belt obtained on a 3D Phoenix v|tome|x s 240 volumetric scanner with a visible manufacturing error: a) in factory condition, before damage, b) with inserted penetrators, c) after removing the penetrators (visible external damage to the rubber layers).

Once the penetrators that caused the tire puncture are removed, the normal repair procedure is to fill the damaged area. The damage to the tire belt, which is clearly visible on the magnification shown in Figure 10, indicates that such a repair method may not restore the original properties of the tire.

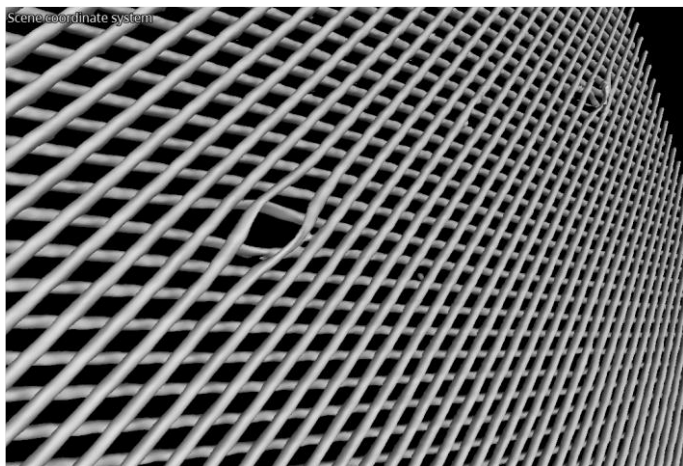


Fig. 10. Magnification of the area of belt damage caused by a tire puncture.

A damaged belt reduces the radial stiffness and thus may affect the outer geometry of the tire. Tires used at high speeds

(driving on motorways) will be particularly vulnerable to this phenomenon. The tire manufacturer dedicates a given structure to be used at certain maximum speeds. Incorrectly diagnosed tire damage may result in a potential operating risk due to tire repair. Externally, the tire will look functional, while its internal damage increases the risk during its use in the vehicle.

The tire belt structure testing method used in this work also allows for more detailed images showing selected fragments. An example of a belt scan showing details of the cord weave is shown in Figure 11.

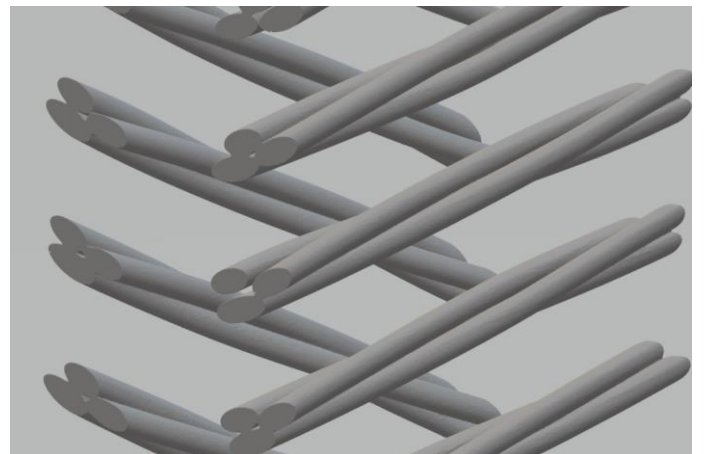


Fig. 11. Result of a scan of the summer tire belt showing details of the cords.

The above belt image was obtained by increasing the number of individual images to 2475 while reducing the distance to the radiation source.

4. Conclusions

Methods of testing complex composite spatial structures are being constantly developed. An interesting example of a commonly used object with such characteristics is the modern car tire. Tests in the field of tire quality control are currently most often carried out on the basis of X-ray devices, by which pictures of the belts are taken. In such methods, applications that enable the automated analysis of the obtained images are crucial. The limitation of these methods is that only a flat representation of the structural component of the tire structure is possible.

The research results presented in the paper allowed for the following conclusions to be formulated:

1. According to the authors, it is advisable to develop the tire quality control methods enabling spatial analysis

of the belt cords. X-ray tomography presented in the article gives such possibilities.

2. In addition to a detailed analysis of tire manufacturing defects, the presented method is perfect for assessing the current technical condition of the belt. A typical example of the need to verify the tire's belting is mechanical damage caused by a puncture. As of today, such tires are qualified for repair in a rather subjective way.
3. Computed tomography allows assessing the extent of belt damage caused by the indentation of the tire structure. On this basis, objective decisions can be made regarding the reparability of the tire and its return to use. A tire after removing the leak but without verifying internal mechanical damage may be a potential hazard during use.

The results presented in this paper are an introduction to further work on the implementation of computed tomography technology in research on tires commonly used in means of transport.

References

1. Anuncia S. M., Saravanan R.: Non-destructive Testing using Radiographic Images - A Survey. *Insight*, Vol. 48, No. 10, 2006, pp. 592-597. DOI:10.1784/insi.2006.48.10.592
2. Brol S., Czok R., Mroz P.: Control of energy conversion and flow in hydraulic-pneumatic system, (2020) *Energy*, 194, art. no. 116849, <https://doi.org/10.1016/j.energy.2019.116849>
3. Brol S., Mamala J.: Application of spectral and wavelet analysis in power train system diagnostic, (2010) *SAE Technical Papers*. <https://doi.org/10.4271/2010-01-0250>. <https://doi.org/10.4271/2010-01-0250>
4. Brol S., Szegda A.: Magnetism of automotive wheels with pneumatic radial tires, (2018) *Measurement: Journal of the International Measurement Confederation*, 126, pp. 37-45. <https://doi.org/10.1016/j.measurement.2018.05.034>
5. Brol S., Warczek J.: Utilization of magnetic signature of automotive tire for exploitational wear assessment. *DIAGNOSTYKA*, 2022, Vol. 23, No. 4. DOI: <https://doi.org/10.29354/diag/156255>
6. Carmignato S., Aloisi V., Medeossi F., Zanini F., Savio E.: Influence of surface roughness on computed tomography dimensional measurements. *CIRP Annals - Manufacturing Technology* 66 (2017). P. 499-502. <https://doi.org/10.1016/j.cirp.2017.04.067>
7. Clark S.K. et al. *Mechanics of Pneumatic Tires*. National Bureau of Standards, U.S. Department of Commerce. 1971.
8. Clark S.K. et al. *The Pneumatic Tire*. U.S. Department of Transportation, National Highway Traffic Safety Administration. February 2006
9. De Chiffre L., Carmignato S., Kruth J.-P., Schmitt R., Weckenmann A.: Industrial applications of computed tomography. *CIRP Annals - Manufacturing Technology* 63 (2014). P. 655-677. <https://doi.org/10.1016/j.cirp.2014.05.011>
10. Egbert A.: High-Resolution X-Ray CT for 3D Failure Analysis and Metrology, FOP:s vårkonferens 2012, Sandviken/SWEDEN
11. Fei Wang: Enhanced Tire Quality Controls by Novel X-ray Digital Detectors. *NDT Technician Newsletter*, Vol. 16, No. 1, pp: 8-11
12. Grzesik W., Brol S.: Identification of surface generation mechanisms based on process feed-back and decomposition of feed marks. (2011) *Advanced Materials Research*, 223, pp. 505-513. <https://doi.org/10.4028/www.scientific.net/AMR.223.505>

13. Guo Zhao, Shiyin Qin: High-Precision Detection of Defects of Tire Texture Through X-ray Imaging Based on Local Inverse Difference Moment Features. *Sensors* 2018, 18(8), 2524; <https://doi.org/10.3390/s18082524>
14. Hermena S., Young M.: CT-scan Image Production Procedures, National Center for Biotechnology, 2022. <https://www.ncbi.nlm.nih.gov/books/NBK574548/>
15. Hongxia Sun, Naijie Gu, Chuanwen Lin: Tire Impurity Defect Detection Based on Grayscale Correction and Threading Method. 2021 IEEE the 6th International Conference on Computer and Communication Systems. 978-0-7381-2604-3/21/ 2021 IEEE. DOI:10.1109/ICCCS52626.2021.9449103
16. Jantos J., Brol S., Mamala J.: Problems in assessing road vehicle driveability parameters determined with the aid of accelerometer. (2007) SAE Technical Papers. <https://doi.org/10.4271/2007-01-1473>.
17. Jazar R. N.: *Vehicle Dynamics: Theory and Application*. Springer, Boston, MA. 2008. <https://doi.org/10.1007/978-0-387-74244-1>
18. Kruth J.P., Bartscher M., Carmignato S., Schmitt R., De Chiffre L., Weckenmann A.: Computed tomography for dimensional metrology. *CIRP Annals - Manufacturing Technology* 60 (2011). P. 821-842. <https://doi.org/10.1016/j.cirp.2011.05.006>
19. Mamala J., Brol S., Graba G.: Hardware-in-the-loop type simulator of spark ignition engine control unit, (2013) International Symposium on Electrodynamic and Mechatronic Systems, SELM 2013 - Proceedings, , art. no. 6562970 , pp. 41-42. DOI:10.1109/SELM.2013.6562970
20. Mamala J.J., Brol S., Jantos J.: The estimation of the engine power with use of an accelerometer, (2010) SAE Technical Papers. <https://doi.org/10.4271/2010-01-0929>.
21. Moj K., Robak G., Owsiniński R., Kurek A., Żak K., Przysiężniuk D.: A new approach for designing cellular structures: design process, manufacturing and structure analysis using a volumetric scanner. *Journal of Mechanical Science and Technology* 37 (3) 2023, p. 1113-1118. <https://doi.org/10.1007/s12206-022-2107-1>
22. Nieslony P., Krolczyka G. M., Wojciechowski S., Chudya R., Żak K., Maruda R. W.: Surface quality and topographic inspection of variable compliance part after precise turning. *Applied Surface Science* 434. 2018. p. 91-101. <https://doi.org/10.1016/j.apsusc.2017.10.158>
23. Praznowski K., Brol S., Augustynowicz A.: Identification of static unbalance wheel of passenger car carried out on a road, (2014) *Solid State Phenomena*, 214 , pp. 48-57. <https://doi.org/10.4028/www.scientific.net/SSP.214.48>
24. Qiang Guo, Caiming Zhang, Hui Liu, Xiaofeng Zhang: Defect Detection in Tire X-Ray Images Using Weighted Texture Dissimilarity. *Journal of Sensors*. Volume 2016, Article ID 4140175, 12 pages. <https://doi.org/10.1155/2016/4140175>
25. Qidan Zhu, Xiaotian Ai: The Defect Detection Algorithm for Tire X-ray Images Based on Deep Learning. 2018 3rd IEEE International Conference on Image, Vision and Computing. 978-1-5386-4991-6/18/\$31.00 2018 IEEE. DOI: 10.1109/ICIVC.2018.8492908
26. Ratajczyk E.: X-ray computed tomography for industrial tasks. *Pomiary Automatyka Robotyka* vol. 5. 2012. P. 104-113.
27. Saberironaghi A., Ren J., El-Gindy M.: Defect Detection Methods for Industrial Products Using Deep Learning Techniques: A Review. *Algorithms* 2023, 16, 95. <https://doi.org/10.3390/a16020095>
28. Valavanis I., Kosmopoulos D.: Multiclass Defect Detection and Classification in Weld Radiographic Images using Geometric and Texture Features. *Expert Systems with Applications*, Vol. 37, No. 12, 2010, pp. 7606-7614. <https://doi.org/10.1016/j.eswa.2010.04.082>
29. Warczek J., Burdzik R., Konieczny Ł., Siwiec G. Frequency analysis of noise generated by pneumatic wheels. *Archives of Acoustics*. Volume 42, Issue 3, Pages 459 - 467. 2017. DOI 10.1515/aoa-2017-0048
30. Xin Yi, Chen Peng, Zhen Zhang, Liang Xiao: The defect detection for X-ray images based on a new lightweight semantic segmentation network. *Mathematical Biosciences and Engineering* Volume 19, Issue 4, 4178-4195. DOI: 10.3934/mbe.2022193
31. Yan Zhang, Dimitri Lefebvre, Qingling Li: Automatic Detection of Defects in Tire Radiographic Images. *IEEE TRANSACTIONS ON AUTOMATION SCIENCE AND ENGINEERING*, VOL. 14, NO. 3, JULY 2017. DOI: 10.1109/TASE.2015.2469594
32. Yan Zhang, Li Tao, Li Qing-Ling: Detection of Foreign Bodies and Bubble Defects in Tire Radiography Images Based on Total Variation and Edge Detection. *Chinese Physics Letters*, Vol. 30, No. 8, 2013. DOI:10.1088/0256-307X/30/8/084205
33. Yilin Wang , Yulong Zhang, Li Zheng, Liedong Yin, Jinshui Chen, Jianguang Lu: Unsupervised Learning with Generative Adversarial Network for Automatic Tire Defect Detection from X-ray Images. *Sensors* 2021, 21(20), 6773; <https://doi.org/10.3390/s21206773>
34. Ying Li, Binbin Fan, Weiping Zhang, Zhiqiang Jiang: A high recall rate method for practical application of tire defect type classification.

Future Generation Computer Systems 125 (2021) 1-9. <https://doi.org/10.1016/j.future.2021.06.009>

35. Zeju Wu, Jiajia Lin, Wenjing Liu: Joint inspection in X-ray #0 belt tire based on periodic texture. *Multimedia Tools and Applications* (2019) 78:9299-9310 <https://doi.org/10.1007/s11042-018-6507-2>
36. Zhouzhou Zheng, , Sen Zhang, Bin Yu, Qingdang Li, Yan Zhang: Defect Inspection in Tire Radiographic Image Using Concise Semantic Segmentation Digital Object Identifier. *IEEE Access* 10.1109/ACCESS.2020.3003089 DOI: 10.1109/ACCESS.2020.3003089